

# Transition-Metal Nanocluster Catalysts: *Scaled-up* Synthesis, Characterization, Storage Conditions, Stability, and Catalytic Activity before and after Storage of Polyoxoanion- and Tetrabutylammonium-Stabilized Ir(0) Nanoclusters

Brooks J. Hornstein and Richard G. Finke\*

Department of Chemistry, Colorado State University, Fort Collins, Colorado 80523

Received August 21, 2002. Revised Manuscript Received November 26, 2002

Previously, we reported the milligram-scale synthesis of tetrabutylammonium- and polyoxoanion ( $\text{P}_2\text{W}_{15}\text{Nb}_3\text{O}_{62}^{9-}$ )-stabilized Ir(0) nanoclusters. To increase the isolable yield of this nanocluster catalyst material to near 1 g, experiments were carried out optimizing the key synthetic variables including the solvent, the presence or absence of olefin during the nanocluster formation reaction, the isolation procedure, and the storage conditions. The ability to quantitatively monitor each nanocluster synthesis by the catalytic activity of the resultant material has led to an optimized synthesis yielding  $880 \pm 10$  mg of  $3.8 \pm 0.6$  nm Ir(0) $_{\sim 2000}$  nanoclusters. The scaled-up nanoclusters are characterized by TEM, elemental analysis, GC, TGA/MS, IR,  $^1\text{H}$ , and  $^{31}\text{P}$  NMR, resulting in compositionally well-characterized nanoclusters with an average stoichiometry of  $[(n\text{-C}_4\text{H}_9)_4\text{N}]_{\sim 11000}\text{Na}_{\sim 5000}\text{Ir}_{\sim 2000}(\text{P}_4\text{W}_{30}\text{Nb}_6\text{O}_{123})_{\sim 1000}(\text{C}_4\text{H}_6\text{O}_3)_{\sim 5000}$  (where  $\text{C}_4\text{H}_6\text{O}_3$  = propylene carbonate). The isolated nanoclusters are active cyclohexene hydrogenation catalysts, possessing  $\sim 65\%$  of their as-formed catalytic activity even after isolation; we have also applied our recently developed  $\text{CS}_2$ -poisoning method to determine the true number of catalytically active sites and thus the true turnover frequency (TOF) in the scaled-up nanoclusters, a rare but valuable number for any nanocluster catalyst. The isolated nanoclusters maintain their activity to within  $\pm 15\%$  for 6 weeks when stored as a solid in a  $\leq 5$  ppm, nitrogen-filled drybox. However, a longer term storage and stability study, the first of its kind, shows that the activity of the scaled-up nanoclusters does decrease by 90% after almost three-fourths of a year (253 days) for an average loss of 2.5% of activity/week, despite the presence of the current “Gold Standard” nanocluster-stabilizing anion,  $\text{P}_2\text{W}_{15}\text{Nb}_3\text{O}_{62}^{9-}$ , and even though the nanoclusters are in the solid-state, are double-bottled, and are in a  $\leq 5$  ppm  $\text{O}_2$  drybox. TEM studies of the resultant material show that agglomeration is not the cause of the deactivation process; instead, a surface deactivation process is implicated, possibly the nanoclusters titrating the  $\leq 5$  ppm  $\text{O}_2$  out of the drybox atmosphere. The nanoclusters are, however, more stable when stored under 40 psig  $\text{H}_2$ , another valuable finding. The results point toward the needed studies of nanocluster surface structures under  $\text{H}_2$ ,  $\text{N}_2$ ,  $\text{O}_2$ , olefins, and other such reagents and ligands. Finally, three lines of evidence are provided indicating that the previously elucidated slow, continuous nucleation and then fast autocatalytic surface-growth nanocluster mechanism of formation also operates in the present synthesis. This in turn means that the multiple insights from that mechanism should also be applicable to the present, scaled-up Ir(0) $_{\sim 2000}$  nanocluster synthesis.

## Introduction

There is considerable interest in the synthesis, characterization, and practical applications of particles  $\leq 10$  nm in diameter, so-called “nanoclusters” or “nanoparticles”.<sup>1</sup> Particles in this size regime lie between the extremes of single-atom species and bulk material; nanoclusters also have a high percentage of their metal atoms on the surface (e.g., 50% of the metal atoms are on the surface of a 2.0-nm nanocluster) and are distinct in key respects from traditional colloids in eight iden-

tifiable ways.<sup>2</sup> Nanoclusters have, therefore, unique chemical and physical characteristics that offer important opportunities for both fundamental studies as well as practical applications.<sup>3</sup>

One exciting area of nanocluster chemistry is in catalysis. If transition-metal nanoclusters can be made

\* To whom correspondence should be addressed. E-mail: rfinke@lamar.colostate.edu.

(1) (a) Aiken, J. D., III; Lin, Y.; Finke, R. G. *J. Mol. Catal. A: Chem.* **1996**, *114*, 29–51. (b) Aiken, J. D., III; Finke, R. G. *J. Mol. Catal. A: Chem.* **1999**, *145*, 1–44. (c) Finke, R. G. Transition-Metal Nanoclusters: Solution-Phase Synthesis, then Characterization and Mechanism of Formation, of Polyoxoanion- and Tetrabutylammonium-Stabilized Nanoclusters. In *Metal Nanoparticles: Synthesis, Characterization and Applications*; Feldheim, D. L., Foss, C. A., Jr., Eds.; Marcel Dekker: New York, 2002; Chapter 2, pp 17–54.

sufficiently stable, catalytically active and long-lived *in solution*, then transition-metal nanoclusters hold considerable promise for serving as soluble analogues of traditional heterogeneous catalysts.<sup>1a</sup> Toward this end, we previously reported the synthesis, full characterization, mechanism of formation, and applications in catalysis of a new subclass of high-stability and high catalytic activity transition-metal nanoclusters, namely,  $P_2W_{15}Nb_3O_{62}^{9-}$ - and  $n-(C_4H_9)_4N^+$ -stabilized  $2.0 \pm 0.3$  nm Ir(0)<sub>190</sub>–Ir(0)<sub>450</sub> nanoclusters.<sup>4–6</sup>

Despite these advances, plus those provided by other groups studying nanoclusters in catalysis,<sup>1b</sup> an important, generally unsolved issue is the *scale-up problem*: the reproducible synthesis and full characterization of isolable, near-monodisperse distributions (i.e.,  $\leq \pm 15\%$  size distributions) of nanoclusters on  $\sim 1$  g or larger scales, followed by studies of their physical properties of interest (in this case, their catalytic activity) and their stability before and after isolation. Indeed, a recent article on nanosized materials concluded with the following view: "Nothing impacts society unless it is scaled up. You have to be able to scale-up..."<sup>7</sup> A 1996 nanocluster workshop also concluded that "the mgs of specific nanoparticles...(currently) available...is simply not enough for economically viable applications" (see p 575 elsewhere<sup>3d</sup>).

The prior literature reporting scaled-up syntheses of transition-metal nanoclusters is limited to that of the following: (a) Moiseev and co-workers' pioneering work on Pd<sub>~560</sub> clusters (made on a 1-g scale);<sup>8</sup> (b) Schmid and co-workers' analogous Pd nanoclusters (made on a 2.3-g Pd(OAc)<sub>2</sub> scale);<sup>9</sup> (c) Bönemann and co-workers' aluminum-organic-stabilized Pt nanoclusters that yield 2.4 g of isolable material;<sup>10</sup> and (d) Bönemann and co-workers' reduction of  $MX_n^-$  with  $R_3BH^-$ , made on 0.5–10-g scales<sup>11,12</sup> (the clear winner presently in terms of larger scale syntheses). However, the  $R_3BH^-$  reductant-based syntheses typically result in compositionally

poorly characterized, boron-contaminated colloids;<sup>2</sup> in addition, the crucial nanocluster-stabilizing anionic component  $X^-$  from the  $MX_n^-$  precursor is largely uncontrolled and sometimes even ignored in these  $R_3BH^-$ -based syntheses (e.g., in the report of "[Ti·0.5THF]<sub>x</sub>"<sup>13</sup>). There is also (e) Bradley's study that specifically addresses the scale-up problem for polymer-stabilized Rh and Pt nanoclusters.<sup>14</sup> However, that work also yields poorly compositionally characterized and probably HCl-contaminated nanocolloids, particles which have  $\sim 2$  times broader size distribution ( $\pm 30\%$ ) than the desired near-monodisperse nanoclusters. Other papers that also recognize the scale-up problem include the following: (f) Klabunde's recent synthesis of Au colloids by the solvated metal-atom dispersion method that claims, in the title, "Gram Scale Synthesis...", but is carried out on a 200-mg scale and leads to only 20 mg of isolated material;<sup>15</sup> (g) Kimura's synthesis that claims "large-scale synthesis of carboxylate-modified Au nanoparticle powders," but where only 128 mg of material is isolated;<sup>16</sup> and (h) Liu's "Quantity Synthesis..." of polymer-stabilized Pt colloids that produces 1 g of material, which, however, is characterized only by TEM.<sup>17</sup> In addition to the literature presented in (a)–(h) above, there are several papers with claims and predictions of scaled-up syntheses,<sup>18</sup> but in each case, the large-scale synthesis of well-characterized nanoclusters remains undemonstrated.

Scrutiny of the nanocluster literature reveals that the following issues, related to the scale-up problem, have yet to be addressed: (i) the choice of the best stabilizing

(2) Modern nanoclusters differ from classical colloids in several important ways. Classic colloids typically (i) are larger in size ( $> 10$  nm), (ii) have broader size distributions ( $> 15\%$ ), (iii) have a poorly defined molecular composition, (iv) are not isolable and redissolvable, (v) are not reproducibly prepared, (vi) have irreproducible catalytic activities (up to 500%), (vii) contain surface-bound, rate-inhibiting species such as  $X^-$ ,  $O^{2-}$ ,  $OH^-$ , and  $H_2O$ , and (viii) historically have been  $H_2O$ , but not organic solvent, soluble.

(3) (a) *Clusters and Colloids: From Theory to Applications*, Schmid, G., Ed.; VCH: New York, 1994. (b) *Physics and Chemistry of Metal Cluster Compounds*, de Jongh, L. J., Ed.; Kluwer Academic Publishers: Dordrecht, 1994; Vol. 18. (c) *Active Metals: Preparation, Characterization, Applications*, Furstner, A., Ed.; VCH: Weinheim, 1996. (d) *Nanoparticles in Solids and Solutions*, Fendler, J. H., Dékány, I., Eds, Kluwer Academic Publishers: Dordrecht, 1996.

(4) Lin, Y.; Finke, R. G. *J. Am. Chem. Soc.* **1994**, *116*, 8335–8353. (5) Watzky, M. A.; Finke, R. G. *J. Am. Chem. Soc.* **1997**, *119*, 10382–10400.

(6) Lin, Y.; Finke, R. G. *Inorg. Chem.* **1994**, *33*, 4891–4910. (7) Dagani, R. Putting the 'Nano' Into Composites. *Chem. Eng. News* **1999**, June 7, 37.

(8) (a) Vargaftik, M. N.; Zagorodnikov, V. P.; Stolyarov, I. P.; Moiseev, I. I.; Likhonolobov, V. A.; Kochubey, D. I.; Chuvilin, A. L.; Zaikovskiy, V. I.; Zamaraev, K. I.; Timofeeva, G. I. *J. Chem. Soc., Chem. Commun.* **1985**, 937–939. (b) Vargaftik, M. N.; Zagorodnikov, V. P.; Stolyarov, I. P.; Moiseev, I. I.; Kochubey, D. I.; Likhonolobov, V. A.; Chuvilin, A. L.; Zamaraev, K. I. *J. Mol. Catal.* **1989**, *53*, 315–348.

(9) Schmid, G.; Haarms, M.; Malm, J.-O.; Bovin, J.-O.; Ruitenbeck, J. van; Zandbergen, H. W.; Fu, W. T. *J. Am. Chem. Soc.* **1993**, *115*, 2046–2048.

(10) Bönemann, H.; Waldofner, N.; Haubold, H.-G.; Vad, T. *Chem. Mater.* **2002**, *14*, 1115–1120.

(11) Bönemann, H.; Brijoux, W.; Brinkmann, R.; Fretzen, R.; Jousen, T.; Koppler, R.; Korall, B.; Neiteler, P.; Richter, J. *J. Mol. Catal.* **1994**, *86*, 129.

(12) Additional references to Bönemann and co-workers' studies: (a) Bönemann, H.; Brijoux, W. *NanoStruct. Mater.* **1995**, *5*, 135. (b) Bönemann, H.; Brinkmann, R.; Neiteler, P. *Appl. Organomet. Chem.* **1994**, *8*, 361. (c) Bönemann, H.; Brinkmann, R.; Koppler, R.; Neiteler, P.; Richter, J. *Adv. Mater.* **1992**, *4*, 804. (d) Bönemann, H.; Brijoux, W.; Brinkman, R.; Dinjus, E.; Fretzen, R.; Jousen, T.; Korall, B. *J. Mol. Catal.* **1992**, *74*, 323. (e) Bönemann, H.; Brijoux, W.; Brinkman, R.; Dinjus, E.; Jousen, T.; Korall, B. *Angew. Chem., Int. Ed. Engl.* **1991**, *30*, 1312–1314.

(13) Franke, R.; Rothe, J.; Pollmann, J.; Hormes, J.; Bönemann, H.; Brijoux, W.; Hindenburg, T. *J. Am. Chem. Soc.* **1996**, *118*, 12090–12097.

(14) (a) An important study demonstrating the need to control the nanocluster-stabilizing anion and associated counteraction (e.g.,  $H^+Cl^-$ ), and showing the irreproducible and greatly reduced catalytic rates that can result if one fails to do so, is Bradley and co-workers' work studying the nanocluster-forming reaction,  $nH^+PtCl_6 + (2n)CH_3OH \rightarrow Pt(0)_n + (2n)HC(O)H + (6n)H^+Cl^-$ .<sup>14b</sup> They showed that if one fails to control the 6 equiv of  $H^+Cl^-$  produced in the reaction, the resultant Pt(0) nanoclusters exhibit a  $\leq 240\%$  variation in their reactivity between preparations and a 350–900% slower rate vs Pt(0) nanoparticles prepared identically, but then subjected to dialysis to remove the excess  $H^+Cl^-$ . [In the absence of dialysis variable amounts of the volatile  $H^+Cl^-$  are lost during the nanocluster drying step under vacuum, resulting in variable catalytic activity.] Impressively, a  $\pm 15\%$  reproducible catalytic activity is achieved, even between different syntheses, when the  $H^+Cl^-$  content of the nanoclusters is controlled during the synthesis of these polymer (poly(vinylpyrrolidone)) protected nanoclusters. As noted elsewhere, the best nanocluster catalyst systems presently available exhibit a homogeneous-catalysis-like,  $\pm 15\%$  reproducible catalytic activity in simple test reactions such as olefin hydrogenation.<sup>1a</sup> (b) Köhler, J.; Bradley, J. S. *Catal. Lett.* **1997**, *45*, 203–208.

(15) Stoeva, S.; Klabunde, K. J.; Sornesen, C. M.; Dragieva, I. J. *Am. Chem. Soc.* **2002**, *124*, 2305–2311.

(16) Chen, S.; Kimura, K. *Langmuir* **1999**, *15*, 1075–1082.

(17) Yu, W.; Liu, H. *Chem. Mater.* **1999**, *10*, 1205.

(18) (a) Yin, Y.; Li, Z.-Y.; Zhong, Z.; Gates, B.; Xia, Y.; Venkateswaran, S. *Mater. Chem.* **2002**, *12*, 552–527. (b) Lu, L.; Wang, H.; Xi, S.; Zhang, H. *J. Mater. Chem.* **2002**, *12*, 156–158. (c) Liao, X.-H.; Zhu, J.-M.; Zhu, J.-J.; Xu, J.-Z.; Chen, H.-Y. *Chem. Commun.* **2001**, 937–938. (d) Tu, W.; Liu, H. *Chem. Mater.* **2000**, *12*, 564–567. (e) Oku, T.; Kusunose, T.; Niihara, K.; Suganuma, K. *J. Mater. Chem.* **2000**, *10*, 255–257. (f) Sun, Y.-P.; Rollins, H. W.; Guduru, R. *Chem. Mater.* **1999**, *11*, 7–9.

solvent (higher dielectric solvents are expected to lead to higher nanocluster stability, *vide infra*; however, a strongly coordinating solvent will hinder catalytic activity by occupying available coordination sites); (ii) the possible effects of the nanocluster isolation procedure (e.g., their precipitation from solution by a less polar solvent such as diethyl ether vs their isolation by simple evaporation of the excess solvent under vacuum); (iii) the thorough characterization of the isolated, scaled-up material produced under optimized conditions; and (iv) the storage and stability properties of the scaled-up and isolated nanoclusters as measured by their desired physical property (in this case their catalytic activity) before and after isolation and as a function of storage time and conditions. That is, can scaled-up syntheses of nanoclusters be isolated with their full, initial catalytic activity in solution intact, or is a loss of activity seen due to processes such as surface deactivation or reconstruction reactions? More subtle issues can be envisaged here as well, for example, the effects of storage under  $H_2$  vs  $N_2$  ( $O_2$  should be avoided as rigorously as possible<sup>19,20</sup>), especially since the heterogeneous catalysis literature indicates that  $H_2$  in sub-surface layer sites may be involved in catalysis.<sup>21</sup> In short, the above four issues surrounding the scaled-up syntheses of nanoclusters, and their resulting stability and catalytic properties, have not been previously addressed.

**Synthesis of Polyoxoanion- and Tetrabutylammonium-Stabilized Nanoclusters on a Near 1-g Scale.** Herein, we report results leading to the optimized synthesis of polyoxoanion-stabilized Ir(0) nanoclusters from the well-defined precursor  $[(n-C_4H_9)_4N]_5-Na_3(1,5-COD)Ir \cdot P_2W_{15}Nb_3O_{62}$ , **1**, in which (i) the nanoclusters are isolated on an 880-mg scale, or (ii) they are stored for up to 30 days *in situ*. We also report (iii) the effects of key synthetic variables such as the solvent, the presence of cyclohexene during the synthesis, and the isolation method, as measured by the catalytic activity before and after isolation and as a function of time and storage conditions (e.g., storage in solution or in the solid state under  $N_2$  vs  $H_2$ ), (iv) characterization of the scaled-up material, including elemental analysis, (v) evidence suggesting that the scaled-up material is formed by the same autocatalytic surface-growth mechanism as our small-scale syntheses,<sup>4,6</sup> and (vi) results of a  $CS_2$ -poisoning experiment that provides the number of sites available for catalysis.

(19) (a) It is already known in the literature,<sup>19b</sup> but less well appreciated than it should be—or simply ignored (see the discussion of this point elsewhere<sup>1a,b</sup>)—that transition-metal(0) nanoclusters are often unstable to  $O_2$  due to the formation of metal-oxide coatings. (b) Kolb, U.; Quaiser, S. A.; Winter, M.; Reetz, M. T. *Chem. Mater.* **1996**, *8*, 1889–1894. (c) Reetz, M. T.; Quaiser, S. A.; Winter, M.; Becker, J. A.; Schafer, R.; Stimming, U.; Marmann, A.; Vogel, R.; Konno, T. *Angew. Chem., Int. Ed. Engl.* **1996**, *35*, 2092. (d) Harada, M.; Asakura, K.; Ueki, Y.; Toshima, N. *J. Phys. Chem.* **1992**, *96*, 9730–9738. (e) See also reference 20(c).

(20) (a) While excessive  $O_2$  often hinders catalysis, smaller amounts of  $O_2$  accelerate Rh hydrogenation catalysis.<sup>20b–d</sup> Hence, in the present work, as in all our past work, to achieve reproducibility we have avoided exposure of our nanoclusters to  $>5$  ppm  $O_2$ , by using a  $N_2$ -filled drybox and sealed Fischer–Porter bottles that attach directly to the hydrogenation line via Swagelok quick-connects (see the Experimental Section). (b) Hamlin, J. E.; Hirai, K.; Gibson, V. C.; Maitlis, P. M. *J. Mol. Catal.* **1982**, *15*, 337–347. (c) Logan, A. D.; Sharoudi, K.; Datye, A. K. *J. Phys. Chem.* **1991**, *95*, 5568, and references therein. (d) A list of early observations of  $O_2$  effects on metal-particle catalysis is given on p 175 of: Maxted, E. B. *Adv. Catal.* **1981**, *3*, 129–179.

Overall, these studies have been successful in providing near-gram amounts of isolable, yet redissolvable, polyoxoanion- and tetrabutylammonium-stabilized  $3.8 \pm 0.6$  nm Ir(0) nanoclusters that exhibit  $\geq 65\%$  of their catalytic activity even after isolation as a solid. These studies also reveal that even Ir(0) nanoclusters from our best scaled-up synthesis steadily lose catalytic activity over several months even when stored as a solid in a  $<5$  ppm  $O_2$ ,  $N_2$ -atmosphere drybox. Hence, our studies emphasize the need to measure the stability of transition-metal nanocluster catalysts by measurements of the desired physical property rather than by solubility alone as has heretofore often been done.<sup>22</sup> The studies that follow also foretell needed surface composition and surface structural studies of transition-metal nanocluster catalysts, work which promises to provide important information about the mechanisms of metal-particle catalyst deactivation.

Last, the present studies are of greater general significance in that the  $P_2W_{15}Nb_3O_{62}^{9-}$  stabilizer herein has been shown to be the presently best anionic stabilizer (the “Gold Standard”) vs other nanocluster-stabilizing anions such as citrate<sup>3-</sup>,  $P_3O_9^{3-}$ , polyacrylate <sup>$n-$</sup> ,  $OAc^-$ ,  $Cl^-$ , and  $OH^-$ .<sup>23</sup> Hence, the issues encountered in scaling up the polyoxoanion-stabilized nanoclusters herein will likely provide even more important when scaling-up nanoclusters which employ other, less stabilizing anions.

## Results and Discussion

Reported below are the results from 22 individual syntheses of polyoxoanion- and tetrabutylammonium-stabilized Ir(0) nanocluster catalysts that were obtained from 108 separate cyclohexene hydrogenation experiments. From these data, an optimized synthesis emerged, one which leads to the production of 880 mg of  $3.8 \pm 0.6$  nm Ir(0) nanoclusters that retain their catalytic activity toward cyclohexene hydrogenation to within  $\pm 15\%$  for up to 6 weeks. A brief discussion of the key variables and their effect on the synthesis of Ir(0) nanoclusters is also provided. These key variables include the solvent, the presence or absence of cyclohexene during the synthesis, and the isolation method. In short, the keys to production of stable and active Ir(0) nanoclusters on a near 1-g scale are their synthesis

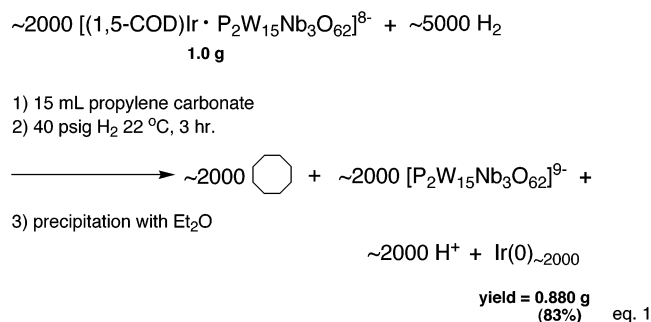
(21) Ceyer, S. T. *Acc. Chem. Res.* **2001**, *34*, 737–744.

(22) Reports that assay nanocluster stability by solubility include the following: (a) Quiros, I.; Yamada, M.; Kubo, K.; Mizutani, J.; Kurihara, M.; Nishihara, H. *Langmuir* **2002**, *18*, 1413–1418. (b) Zhou, Y.; Itoh, H.; Uemura, T.; Naka, K.; Chujo, Y. *Langmuir* **2002**, *18*, 277–283. (c) Kim, H. S.; Ryu, J. H.; Jose, B.; Lee, B. G.; Ahn, B. S.; Kang, Y. S. *Langmuir* **2001**, *17*, 5817–5820. (d) Yu, H.; Gibbons, P. C.; Kelton, K. F.; Buhro, W. E. *J. Am. Chem. Soc.* **2001**, *123*, 9198–9199. (e) Wang, R.; Yang, J.; Zheng, Z.; Carducci, M. D.; Jiao, J.; Seraphin, S. *Angew. Chem., Int. Ed. Engl.* **2001**, *40*, 549–552. (f) Yan, X.; Liu, H.; Liew, Y. *J. Mater. Chem.* **2001**, *11*, 3387–3391. (g) Teranishi, T.; Haga, M.; Shiozawa, Y.; Miyake, M. *J. Am. Chem. Soc.* **2000**, *122*, 4237–4238. (h) Yang, C.-S.; Liu, Q.; Kauzlarich, S. M.; Phillips, B. *Chem. Mater.* **2000**, *12*, 983–988. (i) Wang, Y.; Ren, J.; Deng, K.; Gui, L.; Tang, Y. *Chem. Mater.* **2000**, *12*, 1622–1627. (j) Vidoni, O.; Philippot, K.; Amiens, C.; Chaudret, B.; Balmes, O.; Malm, J.-O.; Bovin, J.-O.; Senocq, F.; Casanove, M.-J. *Angew. Chem., Int. Ed.* **1999**, *38*, 3736–3738. (k) Naka, K.; Yaguchi, M.; Chujo, Y. *Chem. Mater.* **1999**, *11*, 849–851. (l) Yonezawa, T.; Toshima, N.; *J. Chem. Soc., Faraday Trans.* **1995**, *91*, 4111–4119. (m) Lewis, L. N.; Lewis, N. *Chem. Mater.* **1989**, *1*, 106–114.

(23) Özkar, S.; Finke, R. G. *J. Am. Chem. Soc.* **2002**, *124*, 5796–5810.



in the polar, but less coordinating, propylene carbonate,<sup>24</sup> without cyclohexene and then their isolation by precipitation using diethyl ether rather than by evaporation of the solvent under vacuum, the latter leading to nanoclusters that have lost their catalytic activity. The essence of the optimized synthesis is summarized in eq 1.



**Synthesis of  $3.8 \pm 0.6$  nm Ir(0) Nanoclusters on a  $\sim 1$ -g Scale in the Preferred Solvent, Propylene Carbonate.** A total of 16 syntheses were carried out on small scales (20–200 mg of  $[(n\text{-C}_4\text{H}_9)_4\text{N}]_5\text{Na}_3(1,5\text{-COD})\text{Ir} \cdot \text{P}_2\text{W}_{15}\text{Nb}_3\text{O}_{62}$ , **1**) to optimize experimental conditions for the large-scale (1 g, **1**) preparation. Exposure of 1.0 g of **1**, dissolved in 15 mL of propylene carbonate, to 40 psig of  $\text{H}_2$  results in a color change from orange to dark brown and then eventually to a dark blue-black solution characteristic of polyoxoanion-stabilized nanoclusters in solution. After 4 h the pre-catalyst is completely reduced, as judged by the evolution of 1 equiv of cyclooctane (Figure S1, Supporting Information); hence, the reaction was stopped. The completely formed nanocluster catalyst was then transferred into the drybox and isolated by precipitation with diethyl ether. This procedure yields  $880 \pm 10$  mg of isolable Ir(0) nanoclusters, which are effective cyclohexene hydrogenation catalysts (initial rate =  $\{-d\text{H}_2/dt\}_0 = 2.0 \pm 0.3$  mmol of  $\text{H}_2/\text{h}$ ). These results are reproducible over separate batches of pre-catalyst, **1**, and different lots of propylene carbonate.

To reproducibly isolate the catalytically active polyoxoanion-stabilized Ir(0) nanoclusters, attention must be paid to the details of the isolation procedure. In particular, the order of addition in the initial precipitation step, and the number of washings with diethyl ether, were shown to affect the activity of the resulting nanocluster catalyst. A control experiment was carried out in which the reaction solution was added to the diethyl ether. This resulted in a catalyst that was only 48% as active as nanoclusters from the best isolation procedure (i.e., vs the opposite order of addition, diethyl ether added to the reaction solution). It is also important to wash the Ir(0) nanocluster only *once* with diethyl ether after the initial precipitation; see the Experimental Section for details. Three control experiments were carried out in which the Ir(0) nanoclusters were washed twice. In each case, the activity was significantly lower for the twice-washed catalyst ( $0.63 \pm 0.35$  mmol of  $\text{H}_2/\text{h}$ ) vs for the once-washed catalyst ( $2.0 \pm 0.3$  mmol of

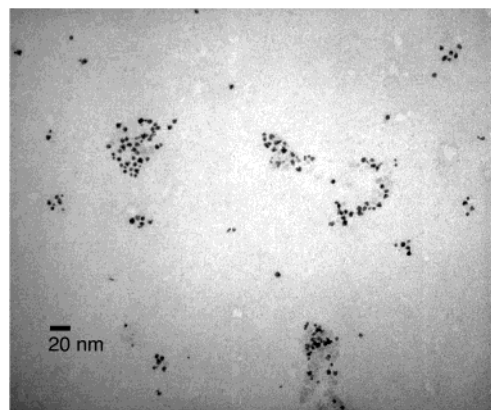


**Figure 1.** TEM image of the scaled-up tetrabutylammonium- and polyoxoanion-stabilized Ir(0) nanoclusters ( $3.8 \pm 0.6$  nm, 120 particles counted).

$\text{H}_2/\text{h}$ ). Excessive washing apparently removes too much of the otherwise nanocluster-stabilizing propylene carbonate.<sup>24,25</sup> These simple but important experimental details demonstrate that the activity of isolated polyoxoanion-stabilized Ir(0) nanocluster catalysts, and probably other nanocluster catalysts, is sensitive to seemingly minor details of the synthesis and the isolation procedure.

**Compositional Characterization of the Scaled-up Ir(0) Nanoclusters.** As discussed in the Introduction, the production of near 1-g quantities of nanocluster material is rare; the compositional characterization of such scaled-up nanoclusters is limited to one prior example.<sup>8</sup> Therefore, the present, scaled-up nanoclusters were characterized by TEM, elemental analysis, GC, TGA/MS, IR,  $^1\text{H}$ , and  $^{31}\text{P}$  NMR.

TEM images of the catalyst material re-suspended in acetonitrile show  $3.8 \pm 0.6$  nm nanoclusters,<sup>26</sup> Figure 1, Ir(0)<sub>~2000</sub> nanoclusters on average. The slightly larger size compared to our previously published synthesis ( $2.0 \pm 0.3$  nm with olefin and  $3.0 \pm 0.4$  nm without olefin<sup>4,6</sup>) is likely a result of the 10-fold higher concentration of the pre-catalyst **1** in the scaled-up synthesis. The composition of the isolated nanoclusters was obtained by elemental analysis, a very classical but still highly valuable technique, one uncommonly used in nanocluster studies.<sup>27</sup> Elemental analysis yields the empirical formula  $\{[(n\text{-C}_4\text{H}_9)_4\text{N}]_{11}\text{Na}_5\text{Ir}_2(\text{P}_4\text{W}_{30}\text{Nb}_6\text{O}_{123})-(\text{C}_4\text{H}_6\text{O}_3)_5\}_x$ . The indicated amount of residual propylene carbonate ( $\text{C}_4\text{H}_6\text{O}_3$ ) in the sample is supported by both TGA/MS and quantitative GC experiments. These data, along with the TEM results, suggest an *average* molecular formula of  $[(n\text{-C}_4\text{H}_9)_4\text{N}]_{\sim 11000}\text{Na}_{\sim 5000}\text{Ir}_{\sim 2000}(\text{P}_4\text{W}_{30}\text{Nb}_6\text{O}_{123})_{\sim 1000}(\text{C}_4\text{H}_6\text{O}_3)_{\sim 5000}$ . Further characterization includes IR and NMR: the IR (KBr pellet) shows bands characteristic of the  $\text{P}_2\text{W}_{15}\text{Nb}_3\text{O}_{62}^{9-}$  polyoxoanion (or its

(25) Fundamental studies are underway, using the methods and five criteria recently developed, examining the relative ability of solvents of high dielectric constant such as propylene carbonate and *N*-methylacetamide for their ability to stabilize transition-metal nanoclusters: Starkey, L.; Finke, R. G., unpublished results and experiments in progress.

(26) Samples for TEM analysis were prepared according to our previously published procedure: Widegren, J. A.; Finke, R. G. *Inorg. Chem.* **2002**, *41*, 1558–1572.

(27) (a) Yonezawa, T.; Onoue, S.-Y.; Kimizuka, N. *Adv. Mater.* **2001**, *13*, 140–142. (b) Yonezawa, T.; Yasui, K.; Kimizuka, N. *Langmuir* **2001**, *17*, 271–273. (c) Perez, H.; Pradeau, J.-P.; Albouy, P.-A.; Perez-Omil, J. *Chem. Mater.* **1999**, *11*, 3460–3463.

(24) Reetz and co-workers were the first to report that propylene carbonate might be a preferred solvent for stabilizing nanoclusters: Reetz, M. T.; Lohmer, G. *J. Chem. Soc., Chem. Commun.* **1996**, 1921–1922.

Nb–O–Nb bridged anhydride,  $P_4W_{30}Nb_6O_{123}^{16-}$ ,<sup>4</sup> tetrabutylammonium, and propylene carbonate, Figure S2, Supporting Information. The  $^1H$  NMR experiment confirms the presence of propylene carbonate in the isolated material in addition to showing signals for the tetrabutylammonium ion, Figure S3, Supporting Information. The  $^{31}P$  NMR shows two groups of signals expected for the two phosphorus nuclei of the polyoxoanion, Figure S4, Supporting Information. Multiple resonances are observed due to the speciation of the stabilizing polyoxoanion that can include free and surface-bound  $P_2W_{15}Nb_3O_{62}^{9-}$  as well as free and surface-bound forms of the Nb–O–Nb bridged anhydride dimer,  $P_4W_{30}Nb_6O_{123}^{16-}$ .<sup>4</sup> Together, these experiments provide one of the best compositionally characterized, *scaled-up* nanocluster systems in the literature. The complete characterization of the all-important *surface* of this or any other nanocluster system remains an important, presently unfulfilled goal, however.

**CS<sub>2</sub> Poisoning of the Scaled-up Ir(0) Nanoclusters.** In addition to the characterization methods described above, we have applied our recently developed nanocluster CS<sub>2</sub>-poisoning method to the scaled-up  $3.8 \pm 0.6$  nm Ir(0) nanoclusters to determine the number of catalytically active sites.<sup>28</sup> The experiment here is conceptually straightforward: the catalytic activity is measured as a function of added aliquots of CS<sub>2</sub> poison, and the typically linear decrease in catalytic activity as a function of the mol of CS<sub>2</sub>/mol of *total* Ir(0) present is extrapolated to its intercept at zero catalytic activity. This crucial CS<sub>2</sub>/Ir(0) ratio allows for a calculation of the *true* turnover frequency (TOF) based on the number of catalytically active sites, all following Boudart's classic work.<sup>29</sup>

A plot of the relative activity vs mol of CS<sub>2</sub>/mol of *total* Ir(0) for the isolated nanoclusters is shown in Figure S5 in the Supporting Information. The data are summarized in Table 1 and lead to at least three important findings. First, only a small amount of CS<sub>2</sub> (0.024 equiv, 2–3% of the *total* Ir(0)) is required to poison >90% of the active Ir(0) catalyst. Second, it is estimated that 7–8% of the *exposed* Ir(0) is catalytically active for cyclohexene hydrogenation under these conditions, an estimate that can jump to as high as 35–40% depending upon how many active Ir(0) each CS<sub>2</sub> poisons.<sup>30</sup> Noteworthy here is that the results are the same, within experimental error, as those from our CS<sub>2</sub>-poisoning studies of polyoxoanion-stabilized Rh(0) nanoclusters.<sup>28</sup> In both cases, the results are best explained by the polyoxoanion binding to the nanoclusters' surface, thereby stabilizing it toward agglomeration but concomitantly inhibiting the nanoclusters' catalytic activity by binding to otherwise catalytically active sites. As pointed out in earlier studies,<sup>28</sup> for polyoxoanion-stabilized nanoclusters, and by Bradley for polymer-stabilized nanoclusters,<sup>31</sup> the increased stabilization of nanoclusters comes

at a cost of catalytic activity. The present CS<sub>2</sub>-poisoning studies, besides providing the best current estimate of the number of active sites present, provide rare data in support of the above increased stabilization/decreased catalytic activity correlation.

**Table 1. Poisoning Results for the Ir(0) Nanoclusters and the Corrected Turnover Frequencies (TOF) at 22 °C**

% Ir(0) on the surface	31% <sup>a</sup>
mol of CS <sub>2</sub> /mol of total Ir(0) required for >90% deactivation	$0.024 \pm 0.006$
mol of CS <sub>2</sub> /mol of exposed Ir(0) required for >90% deactivation	$0.07 \pm 0.02$
TOF (based on total Ir(0))	$56 \text{ h}^{-1}$
TOF (corrected for exposed Ir(0))	$180 \text{ h}^{-1}$
TOF (corrected for active Ir(0) atoms determined by CS <sub>2</sub> poisoning and using a 1/5 CS <sub>2</sub> /Ir stoichiometry <sup>b</sup> )	$470 \text{ h}^{-1}$

<sup>a</sup> Estimated from a "naked" magic number nanocluster of Ir(0)<sub>2057</sub> that corresponds to the experimentally determined size of  $3.8 \pm 0.6$  nm. <sup>b</sup> See elsewhere for a discussion of the single-crystal literature leading to this stoichiometric estimation.<sup>28</sup>

Finally, the small amount of CS<sub>2</sub> required for almost total deactivation (0.024 mol of CS<sub>2</sub>/mol of *total* Ir(0)) cannot be explained by a homogeneous, single-metal-site, Ir<sub>1</sub> catalyst: such a catalyst with  $\geq 1$  site of coordinative unsaturation would require  $\geq 1$  equiv of CS<sub>2</sub> to reach complete deactivation, a value  $\geq 41$  times larger than that experimentally observed. The 0.024 mol of CS<sub>2</sub>/mol of *total* Ir(0) is, however, consistent with and fully supportive of the presence of the true catalyst being a nanocluster catalyst in which  $\gg 50\%$  of the total metal is inaccessible geometrically (i.e., by being in the core of the structure and thus below the surface of the nanocluster). Although the identity of the true catalyst in this system has been well-established in other work to be soluble Ir(0) nanoclusters,<sup>4,6</sup> the present CS<sub>2</sub>-poisoning experiment demonstrates the ability of this kinetics-based method to help distinguish single-metal homogeneous catalysis from multimetallic, metal-particle heterogeneous catalysis: is the ratio  $\geq 1$  or  $\ll 1$ ?<sup>32</sup> A control experiment was also performed showing that, as expected for a nanocluster catalyst, the catalytic activity is first-order in the concentration of nanoclusters, Figure S6. That experiment also shows that the catalytic activities reported herein are free from H<sub>2</sub> gas-to-solution mass-transfer limitations, complications that have been shown to ruin nanocluster syntheses by leading to broad size dispersions.<sup>33</sup>

**Solid-State Storage Properties of the Scaled-up Ir(0) Nanoclusters.** Even though our Ir(0) nanocluster system contains the current "Gold Standard" anion stabilizer,  $P_2W_{15}Nb_3O_{62}^{9-}$ ,<sup>9–23</sup> extended storage in a  $\leq 5$  ppm O<sub>2</sub>, N<sub>2</sub>-filled drybox with the sample double-bottled still leads to 90% deactivation of the catalyst after 253 days, Figure 2, an average loss of 2.5% of catalytic activity/week. TEM evidence, Figure S7 of the Supporting Information, indicates that the deactivation is *not* due to agglomeration; hence, the deactivation is likely a nanocluster surface phenomenon, an issue we can now

(28) Hornstein, B. J.; Aiken, J. D., III; Finke, R. G. *Inorg. Chem.* **2002**, *41*, 1625–1638.

(29) Boudart, M. *Chem. Rev.* **1995**, *95*, 661–666. Boudart, M. *J. Mol. Catal.* **1985**, *30*, 27.

(30) This 7–8% estimate is derived using the 0.024 equiv of CS<sub>2</sub>, a 1/1 ratio of CS<sub>2</sub>/Ir(0) stoichiometry, and the  $3.8 \pm 0.6$  nm size of the isolated nanoclusters, which have 28–34% of the total Ir(0) on the surface. If one uses instead the 1/5 CS<sub>2</sub>/Ir(0) stoichiometry estimated elsewhere,<sup>28</sup> one calculates that 35–40% of the exposed Ir(0) is active.

(31) de Caro, D.; Bradley, J. S. *New J. Chem.* **1998**, *22*, 1267–1273.

(32) (a) Widegren, J. A.; Finke, R. G. A Review of the Problem of Distinguishing True Homogeneous Catalysis From Soluble-Metal-Particle Heterogeneous Catalysis Under Reducing Conditions. *J. Mol. Catal. A: Chem.* **2003**, in press.<sup>32b</sup> (b) Based on a chapter in Jason A. Widegren's Ph.D. dissertation, Colorado State University, Aug 2002.

(33) Aiken, J. D., III; Finke, R. G. *J. Am. Chem. Soc.* **1998**, *120*, 9545–9554.



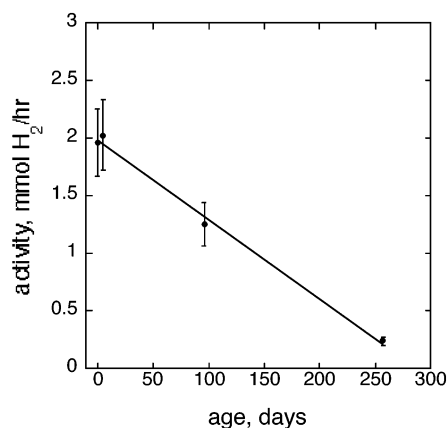


**Figure 2.** Plot of the cyclohexene hydrogenation activity vs time for the scaled-up Ir(0) nanoclusters showing that 90% of the catalytic activity is lost after ca. three-fourths of a year (253 days), an average of 2.5% a week, during storage in a nitrogen-filled,  $\leq 5$  ppm O<sub>2</sub>, 25 °C drybox.

address in a future study since the required scaled-up amounts of nanoclusters are available for study.

It is quite possible that trace O<sub>2</sub> is responsible for the deactivation seen upon storage of the nanoclusters, even though we have taken all possible care to avoid exposure of our nanoclusters to O<sub>2</sub> by storing them double-bottled in a  $\leq 5$  ppm drybox (see the Experimental Section). Back-of-the-envelope calculations show that if the 5 ppm of O<sub>2</sub> in just the 1-L volume of the outer storage bottle is completely scavenged by the Ir(0)<sub>~2000</sub> nanoclusters, this would account for  $\approx 0.4\%$  poisoning of the nanoclusters' surface, a calculation<sup>34</sup> that assumes O<sub>2</sub> is a poison<sup>20</sup> (and a 1:1 O<sub>2</sub>:Ir poison). That is, just 4–8, 1-L volumes of 5 ppm air *may* be able to poison completely the observed, CS<sub>2</sub>-titration determined, 2–3% of active Ir(0). An important conceptual point here is that *nanoclusters of a given transition metal, M, are expected to be much more air-sensitive than the bulk form of that same metal due to the much higher surface area of the nanoclusters, their less negative  $\Delta H_{\text{formation}}$  and, hence, their intrinsically greater reactivity* (e.g., see footnote 28 and Figure 8 elsewhere<sup>35</sup>). Note that the 40 psig of H<sub>2</sub> of the cyclohexene hydrogenation conditions does not reactivate the nanoclusters under at least solution conditions, although it is possible higher pressure or temperature treatments of the nanoclusters as a solid would reactivate them, something we have not yet tested.

Note, however, that even *if* trace O<sub>2</sub> is the cause of the observed deactivation upon storage, it follows that our choice of as O<sub>2</sub>-“free” experimental conditions as possible for the syntheses of our nanoclusters from the beginning<sup>4</sup> (i.e., a drybox-based synthesis) means that the *as-isolated* Ir(0) nanoclusters are largely uncontaminated by O<sub>2</sub>. The experimental evidence for this

is: (a) that the catalytic activity decreases with time so that the initial activity must of course therefore be for the unpoisoned material, and (b) that the reproducibility of the catalytic activity in independent Ir(0) nanocluster syntheses is  $\pm 15\%$ . This level of reproducibility is as high as that typically exhibited by even air-sensitive, small-molecule organometallics, for example, a reproducibility that allows for at most  $\pm 15\%$  effects due to O<sub>2</sub> (and all other contaminants) in the as-isolated catalyst.

An alternative hypothesis for the observed inactivation upon storage is that N<sub>2</sub> interacts with the Ir(0) surface and causes deactivation to occur. Although N<sub>2</sub> does not dissociatively adsorb on Ir(0) at temperatures up to 1000 °C,<sup>36</sup> there is evidence that N<sub>2</sub> increases the density of Ir(0) nanoparticles supported on a TiO<sub>2</sub> surface.<sup>37</sup> The authors note that “N<sub>2</sub> interacts only weakly with Ir(0) crystallites” but this weak interaction may be strong enough to cause deactivation of our Ir(0) nanoparticle catalyst when stored under N<sub>2</sub>. Further investigations of the deactivation mechanism, including a control experiment in which the Ir(0) nanoclusters are stored under argon, are warranted.

In short, the present study is the first to document the deactivation of isolable nanoclusters upon storage in even a  $\leq 5$  ppm O<sub>2</sub>, N<sub>2</sub>-filled drybox. This key finding emphasizes the need to perform and report studies that probe the storage stability of transition-metal nanoclusters. Our results further remind us that the “stability” of nanoclusters over time is best addressed by quantitative measurements of the desired physical property, in our case catalytic activity, rather than only by qualitative indicators of more easily measured, but less relevant, properties such as the often reported solubility or re-dissolvability.<sup>22</sup> The present work is one of only five transition-metal nanocluster papers<sup>38</sup> to address nanocluster stability in a more rigorous manner and one of two that probes the stability with catalytic activity.<sup>39</sup>

Also worth noting here is the point we have made previously:<sup>1b</sup> the O<sub>2</sub> sensitivity of transition-metal nanoclusters is a confused, often ignored, topic<sup>40</sup> that deserves additional, careful, and quantitative scrutiny. *If* trace O<sub>2</sub> is deactivating Ir(0) nanoclusters in even a  $\leq 5$  ppm drybox upon double-bottle storage at the observed rate of 2.5%/week, then this is a very important observation, one that would bear on nearly all past and present, transition-metal nanocluster catalysis. It will also be most interesting and informative to see how scaled-up Rh(0) nanoclusters store since trace O<sub>2</sub> increases hydrogenation rates of Rh metal-particle catalysts,<sup>20</sup> a finding that we have confirmed for at least our earlier Rh nanoclusters.<sup>41</sup>

(36) Nieuwenhuys, B. E.; Somorjai, G. A. *Surf. Sci.* **1978**, *72*, 8–32.

(37) Berkó, A.; Solymosi, F. *J. Phys. Chem. B* **2000**, *104*, 10215–10221.

(38) Both TEM<sup>38b,d</sup> and UV/vis spectroscopy<sup>38a,c-e</sup> have been used to assess the stability of transition-metal nanoclusters. (a) Tzhayik, O.; Sawant, P.; Efrima, S.; Kovalev, E.; Klug, J. T. *Langmuir* **2002**, *18*, 3364–3369. (b) Zhao, S.-Y.; Chen, S.-H.; Wang, S.-Y.; Li, D.-G.; Ma, H.-Y. *Langmuir* **2002**, *18*, 3315–3318. (c) Pastoriza-Santos, I.; Liz-Marzan, L. M. *Langmuir* **2002**, *18*, 2888–2894. (d) Walker, C. H.; St. John, J. V.; Wisian-Neilson, P. *J. Am. Chem. Soc.* **2001**, *123*, 3846–3847. (e) Zhang, Z.; Patel, R. C.; Kothari, R.; Johnson, C. P.; Friberg, S. E.; Aikens, P. A. *J. Phys. Chem. B* **2000**, *104*, 1176–1182.

(39) The in situ stability of polymer-protected Ni/Pd bimetallic nanoclusters in the following study was tested by nitrobenzene hydrogenation activity: (a) Lu, P.; Teranishi, T.; Asakura, K.; Miyake, M.; Toshima, N. *J. Phys. Chem. B* **1999**, *103*, 9673–9682.

(34) The amount of exposed Ir(0) is calculated from the mass of the sample, the percentage of Ir from elemental analysis, and the percentage of exposed metal for an Ir(0)<sub>~2000</sub> nanocluster (i.e., mol of exposed Ir(0) =  $0.880 \text{ g} \times 0.0366 \times 0.30/192 \text{ g/mol} = 5.02 \times 10^{-5} \text{ mol}$  of exposed Ir(0)). The molar amount of O<sub>2</sub> in a single 1-L volume of 5 ppm O<sub>2</sub> drybox atmosphere is calculated from the ideal gas law (i.e., mol of O<sub>2</sub> =  $5/1 \times 10^6 \times (1 \text{ atm} \times 1 \text{ L})/(300 \text{ K} \times 0.082 \text{ L} \times \text{atm/mol} \times \text{K}) = 2.03 \times 10^{-7} \text{ mol}$  of O<sub>2</sub>). Therefore, oxygen is capable of “poisoning”  $2.03 \times 10^{-7}/5.02 \times 10^{-5} \times 100\% = 0.4\%$  of the exposed Ir(0) surface. This estimation assumes that the entire amount of O<sub>2</sub> in the 1-L volume is adsorbed by the nanocluster sample and that the O<sub>2</sub>/Ir(0) stoichiometry is 1/1.

(35) Watzky, M. A.; Finke, R. G. *Chem. Mater.* **1997**, *9*, 3083.

Table 2. Summary and Results of Key Ir(0) Nanocluster Syntheses<sup>a</sup>

exp. no.	mg of 1	solvent	volume of olefin added	isolation method (or in situ)	storage conditions	initial catalytic activity <sup>b</sup> (mmol of H <sub>2</sub> /h)	average catalytic activity <sup>b,c</sup> (mmol of H <sub>2</sub> /h)
<b>1. Most Successful Syntheses</b>							
5	200	propylene carbonate 6.0 mL	0.0	precipitated with Et <sub>2</sub> O	N <sub>2</sub> drybox	2.0 ± 0.6	2.0 ± 0.3
6	1000	propylene carbonate 15.0 mL	0.0	precipitated with Et <sub>2</sub> O	N <sub>2</sub> drybox	2.2 ± 0.3	2.0 ± 0.3 <sup>d</sup>
8	200	propylene carbonate 6.0 mL	0.0	in situ	40 psig H <sub>2</sub>	3.1 ± 0.7	2.4 ± 0.4
3	200	propylene carbonate 6.0 mL	1.2 mL	In situ	40 psig H <sub>2</sub>	2.9 ± 0.2	2.4 ± 0.5
<b>2. In Situ Storage</b>							
8	200	propylene carbonate 6.0 mL	0.0	in situ	40 psig H <sub>2</sub>	3.1 ± 0.7	2.4 ± 0.4
7	115	propylene carbonate 3.5 mL	0.0	in situ	N <sub>2</sub> drybox	3.1 ± 0.7	0.8 ± 0.1 after 4 days
3	200	propylene carbonate 6.0 mL	1.2 mL	in situ	40 psig H <sub>2</sub>	2.9 ± 0.2	2.4 ± 0.5
2	200	propylene carbonate 3.5 mL	1.2 mL	in situ	N <sub>2</sub> drybox	2.9 ± 0.2	1.5 ± 0.3
<b>3. Solvent Effects</b>							
5	200	propylene carbonate 6.0 mL	0.0	precipitated with Et <sub>2</sub> O	N <sub>2</sub> drybox	2.0 ± 0.6	2.0 ± 0.3
12	160	acetone 20.0 mL	0.0	precipitated with Et <sub>2</sub> O	N <sub>2</sub> drybox	2.2 ± 0.6	4.1 ± 1.0
<b>4. Effect of Cyclohexene</b>							
5	200	propylene carbonate 6.0 mL	0.0	precipitated with Et <sub>2</sub> O	N <sub>2</sub> drybox	2.0 ± 0.6	2.0 ± 0.3
1	200	propylene carbonate 6.0 mL	1.2 mL	precipitated with Et <sub>2</sub> O	N <sub>2</sub> drybox <sup>a</sup>	2.6	1.2 ± 0.8 after 1 day
<b>5. Effects of Isolation on the Initial Activity</b>							
5	200	propylene carbonate 6.0 mL	0.0	precipitated with Et <sub>2</sub> O		2.0 ± 0.6 <sup>d</sup>	
7	115	propylene carbonate 3.5 mL	0.0	in situ		3.1 ± 0.7	
<b>6. Isolation Method</b>							
5	200	propylene carbonate 6.0 mL	0.0	precipitated with Et <sub>2</sub> O	N <sub>2</sub> drybox	2.0 ± 0.6	2.0 ± 0.3
4	200	propylene carbonate 6.0 mL	0.0	evaporated to dryness	N <sub>2</sub> drybox	0	0

<sup>a</sup> A comprehensive table of experiments is provided in the Supporting Information, Table S1. <sup>b</sup> Catalytic activity is based on 5.0 mg of catalyst. <sup>c</sup> The "average catalytic activity" for each catalyst was determined from individual experiments carried out over a 45-day period.

<sup>d</sup> This catalyst is 90% deactivated after 253 days of storage as a solid in the drybox.

**In Situ Storage of Ir(0) Nanoclusters under 40 psig H<sub>2</sub> Leads to Stable, Active Ir(0) Nanocluster Catalysts in Propylene Carbonate.** An active and stable catalyst was obtained when the Ir(0) nanoclusters were synthesized under the same conditions as above on a 200-mg scale and then stored in situ under 40 psig H<sub>2</sub>. The activity of this catalyst is the same as the isolated Ir(0) nanoclusters, within experimental error (Table 2, section 1) over a 30-day period. In contrast, in situ storage of the nanocluster sample under N<sub>2</sub> resulted in 74% deactivation of the catalyst after only 4 days, Table 2, section 2.

The positive effects of storage under H<sub>2</sub> were anticipated in light of the possible extreme air sensitivity of the nanoclusters (vide supra) and since a previous study suggests that storage in a reducing medium (glycol) provides stabilization for Ni/Pd nanoclusters in solution

for up to 6 months.<sup>39a</sup> Alternatively, the improved solution storage properties may be due to pre-adsorbed H<sub>2</sub> on the surface of the catalyst, which has been shown by Somorjai et al. to enhance the catalytic activity of a Pt surface.<sup>42</sup> In addition, the interaction of H<sub>2</sub> with metal surfaces is well-documented in the literature and can result in surface reconstruction that may lead to changes in catalytic activity.<sup>43</sup> Although the details of the Ir(0)/H<sub>2</sub> interaction in our system are unknown at present, it is clear that in situ storage under H<sub>2</sub> is superior to storage under N<sub>2</sub> for maintaining the nanoclusters' catalytic activity over time. It is also possible that storage under H<sub>2</sub> may improve the solid-state stability of the nanoclusters as well, although this was not tested since the effective storage time of up to 6 weeks was sufficient for most of our studies, fresh nanoclusters being made anytime a sample had been stored for 6 weeks.

**Key Variables in the Synthesis of Scaled-up Polyoxoanion- and Tetrabutylammonium-Stabilized Ir(0) Nanoclusters as Measured by Cyclohexene Hydrogenation Catalytic Activity. (A) Solvent.** Our initial attempts at scale-up were carried out in acetone, the same solvent used for our initial 3-mg-scale syntheses of polyoxoanion- and tetrabutylammonium-stabilized Ir(0) nanoclusters.<sup>4,6</sup> The Ir(0) nano-

(40) Evidence for Pd–O formation in nanoclusters has appeared: (a) Harada, M.; Asakura, K.; Ueki, Y.; Toshima, N. *J. Phys. Chem.* **1992**, *96*, 9730. (b) Toshima, N.; Harada, M.; Yonezawa, T.; Kushihashi, K.; Asakura, K. *J. Phys. Chem.* **1991**, *95*, 7448. (c) Pd<sub>3</sub>(AOc)<sub>6</sub>(DMSO)<sub>6</sub> (O/OH/OH<sub>2</sub>)<sub>4</sub> nanoclusters (by elemental analysis) in oxidation catalysis: van Benthem, R. A. T. M.; Hiemstra, H.; van Leeuwen, P. W. N. M.; Geus, J. W.; Speckamp, W. N. *Angew. Chem., Int. Ed. Engl.* **1995**, *34*, 457. (d) Electrochemically prepared Pd nanoclusters that are claimed to not be O<sub>2</sub>-sensitive have been reported, although it is unclear if the sample analyzed was exposed to air; moreover, such claimed air insensitivity seems inconsistent with the other, available literature on Pd or Pd/Pt nanoclusters:<sup>a–c</sup> Reetz, M. T.; Heilbeig, W. *J. Am. Chem. Soc.* **1994**, *116*, 7401. (e) One careful study of the O<sub>2</sub> oxidation of Co nanoclusters is available: Reetz, M. T.; Quaiser, S. A.; Winter, M.; Becker, J. A.; Schäfer, R.; Stimming, U.; Marmann, A.; Vogel, R.; Konno, T. *Angew. Chem., Int. Ed. Engl.* **1996**, *35*, 2092. (f) As a recent case in point that more attention needs to be paid to the potential air sensitivity of transition-metal nanoclusters, a collaborative paper from five laboratories, attempting to understand the different nanocluster catalysts, *did not* control exposure to O<sub>2</sub> as a part of those studies: Toshima, N.; Shiraishi, Y.; Teranishi, T.; Miyake, M.; Tominaga, T.; Watanabe, H.; Brijoux, W.; Bönemann, H.; Schmid, G. *Appl. Organomet. Chem.* **2001**, *15*, 178.

(41) Edlund, D. Ph.D. Thesis, University of Oregon, Sept 1987. See Table 4, p 197, and Table 5, p 200 (O<sub>2</sub> effects on Rh(0)<sub>n</sub> hydrogenation catalysis).

(42) Wieckowski, A.; Rosasco, S. D.; Salaita, G. N.; Hubbard, A.; Bent, B. E.; Zaera, F.; Godbey, D.; Somorjai, G. A. *J. Am. Chem. Soc.* **1985**, *107*, 5910–5920.

(43) (a) Ferri, D.; Bürgi, T.; Baiker, A. *J. Phys. Chem. B* **2001**, *105*, 3187–3195. (b) Choukroun, R.; de Caro, D.; Chaudret, B.; Lecante, P.; Snoeck, E. *New J. Chem.* **2001**, *25*, 525–527. (c) Teeter, G.; Hinson, D.; Erskine, J. L. *Phys. Rev. B* **1998**, *57*, 4073–4080. (d) Arnold, M.; Sologub, S.; Frie, W.; Hammer, L.; Heinz, K. *J. Phys. Condens. Matter* **1997**, *9*, 6481–6491. (e) Tománek, D.; Wilke, S.; Scheffler, M. *Phys. Rev. Lett.* **1997**, *79*, 1329–1332. (f) Somorjai, G. A. *Annu. Rev. Phys. Chem.* **1994**, *45*, 721–751. (g) *Hydrogen Effects in Catalysis: Fundamentals and Practical Applications*; Paál, Z.; Menon, P. G., Eds.; Marcel Dekker: New York, 1988.

clusters isolated from acetone show a somewhat erratic catalytic activity, one that can vary by 100% between experiments, Figure S8. The reproducibility of the catalytic activity in acetone is clearly poorer than the  $\pm 15\%$  reproducibility in propylene carbonate as a comparison of Figures S8 (acetone) and S9 (propylene carbonate) shows. The high variability in acetone is probably why the *initial activity* (measured immediately after isolation) *appears* to be different than the *average activity* (calculated for each sample from individual experiments carried out over a 45-day period) in Table S1 of the Supporting Information—that is, the large variability and accompanying large error bars probably mean that the initial and average activities in acetone are the same within the (large) error observed. The use of propylene carbonate also avoids the premature precipitation of the catalyst, which is often observed in nanocluster syntheses carried out in acetone and has been attributed to the increasing concentration of the less-polar product, cyclohexane, resulting from cyclohexene hydrogenation. In short, the higher dielectric solvent, propylene carbonate, is superior to acetone for the  $\sim 1$ -g-scale syntheses of polyoxoanion- and tetrabutylamminium-stabilized Ir(0) nanoclusters under the conditions employed. This is a valuable finding since the use of high dielectric solvents for improved stability of nanoclusters is just beginning to be appreciated in the nanocluster area,<sup>23–25</sup> despite the established value of higher dielectric media in stabilizing classical colloids.<sup>44</sup>

**(B) Effect of the Olefin, Cyclohexene, on the Synthesis of Polyoxoanion-Stabilized Ir(0) Nanoclusters.** Our initial small-scale synthesis of Ir(0) nanoclusters in acetone *requires* cyclohexene for the formation of near-monodisperse  $2.0 \pm 0.3$  nm Ir(0) nanoclusters; in the absence of olefin, larger  $3.0 \pm 0.4$  nm Ir(0) nanoclusters are formed.<sup>4</sup> Moreover, the hydrogenation of cyclohexene serves as a reporter reaction for the formation of our polyoxoanion-stabilized nanoclusters.<sup>5,45</sup> Our ability to quantitatively follow this reaction has led to a detailed mechanistic description of nanocluster nucleation and growth, which is proving to be general for the formation of transition-metal nanoclusters from the reduction of metal salt precursors.<sup>5,45</sup> Hence, we tested the effects of the presence of cyclohexene on the scaled-up synthesis.

Despite the benefits of cyclohexene in our small-scale syntheses carried out in acetone, its presence in larger scale experiments in propylene carbonate leads to *rapid catalyst deactivation*. For example, the catalytic activity drops from an initial value of 2.6 mmol of H<sub>2</sub>/h to 1.2 mmol of H<sub>2</sub>/h after only 1 day, Table 2, section 4. It is clear from this experiment that olefins such as cyclohexene should be avoided, at least when the synthesis is carried out under our conditions. Although not previously reported in the nanocluster area, there is precedent for olefin-based formation of allyl, vinyl, and alkylidene species atop the surfaces of heterogeneous catalysts, ligands which can act as catalyst poisons.<sup>46</sup> Indeed, for the case of ethylene hydrogenation by

supported Ir<sub>4</sub> nanoclusters, Gates has shown that spectator ligands include  $\pi$ -bonded ethene, di- $\sigma$ -bonded ethene, and ethylidyne.<sup>47</sup>

**(C) Effects of Isolation and Isolation Method on the Catalytic Activity.** To determine if isolation of the nanocluster catalyst from propylene carbonate results in a significant decrease in activity, the catalytic activity was measured before ( $3.1 \pm 0.7$  mmol of H<sub>2</sub>/h) and then immediately after ( $2.0 \pm 0.6$  mmol of H<sub>2</sub>/h) isolation of the Ir(0) nanoclusters by precipitation with diethyl ether. Even for Ir(0) nanoclusters made under the optimized conditions, the catalytic activity decreased by 35% upon isolation (Table 2, section 5), mostly likely due to some level of surface restructuring, for example, the conversion of adatom, kink, or step sites to sites of less coordinative unsaturation. Worth noting here is that the *isolation method does matter*. If the propylene carbonate solvent is removed under reduced pressure at 80 °C, the resulting Ir(0) nanoclusters are *inactive* toward cyclohexene hydrogenation, Table 2, section 6. This inferior procedure also has the disadvantage of requiring >24 h. In short, isolation of the nanocluster catalyst by precipitation with Et<sub>2</sub>O is the most effective procedure for obtaining stable, storable, active Ir(0) nanoclusters. This is the first quantitative comparison of nanocluster catalytic activity before and after isolation. Clearly, studies of the desired physical property before and after nanocluster isolations are important for the eventual larger scale production and use of nanocluster materials. Hence, testing the possible generality of this result is an important experiment for other nanocluster systems and applications.

**Verification of the Autocatalytic Surface-Growth Mechanism for Ir(0) Nanoclusters in Propylene Carbonate.** The autocatalytic, surface-growth mechanism leads to the formation of near-monodisperse transition-metal nanoclusters under reducing agents such H<sub>2</sub>.<sup>4–6</sup> Although this mechanism is well-established for reactions in acetone/cyclohexene, it had not been demonstrated in propylene carbonate alone. By using a sensitive H<sub>2</sub>-gas uptake apparatus (Figure S10, Supporting Information), we were able to obtain strong support for this mechanism under the optimized synthetic conditions (see the Supporting Information for further details of the following experiments). This evidence includes the following: (i) the consumption of the previously documented<sup>4–6</sup> 3.5 equiv of H<sub>2</sub>/mol of **1** according to Scheme 1; (ii) the sigmoidal shape of the H<sub>2</sub> consumption curve (Figure S11, Supporting Information); and (iii) the evolution of 1 equiv of cyclooctane (Figure S12, Supporting Information). By comparison to the published diagnostics for the slow, continuous nucleation, then autocatalytic surface-growth mechanism, these results provide compelling evidence that this mechanism is operative in propylene carbonate as well as in acetone.<sup>5</sup> Scheme 1 summarizes some of the established steps,<sup>4–6,45</sup> which lead to the observed

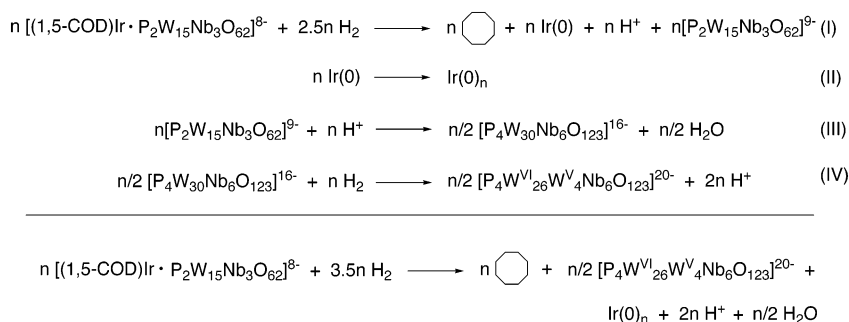
(44) Evans, D. F.; Wenneström, H. *The Colloidal Domain: Where Physics, Chemistry, Biology and Technology Meet*, 2<sup>nd</sup> ed.; Wiley-VCH: New York, 1999.

(45) Widegren, J. A.; Aiken, J. D., III; Ozkar, S.; Finke, R. G. *Chem. Mater.* **2001**, *13*, 312–324.

(46) (a) Stacchiola, D.; Azad, S.; Burkholder, L.; Tysoe, W. T. *J. Phys. Chem. B* **2001**, *105*, 11233–11239. (b) Jacobs, P. W.; Somorjai, G. A. *J. Mol. Catal. A* **1998**, *131*, 5–18. (c) Zaera, F. *Langmuir* **1996**, *12*, 88–94. (d) Somorjai, G. A. Surface chemistry on the nanometer scale. *Proc. Robert A. Welch Found. Conf. Chem. Res.* **1996**, *40*, 57–85.

(47) Argo, M. A.; Odzak, J. F.; Lai, F. S.; Gates, B. C. *Nature* **2002**, *415*, 623.



**Scheme 1. Precedented,<sup>4,5</sup> Balanced Reactions for the Formation of Ir(0) Nanoclusters from 1<sup>a</sup>**

<sup>a</sup> The uptake of 3.5 equiv of H<sub>2</sub>, the sigmoidal nanocluster formation kinetics (Figure S10), and the evolution of 1.0 equiv of cyclooctane support the application of the autocatalytic mechanism to the present case. Additional results supporting this mechanism are available elsewhere<sup>4,5</sup> and include evidence for the formation of the Nb–O–Nb, anhydride bridged  $\{(\text{P}_2\text{W}_{15}\text{Nb}_3\text{O}_{61})_2\text{O}\}^{16-}$  ( $=\text{P}_4\text{W}^{\text{VI}}_{30}\text{Nb}_6\text{O}_{123}^{16-}$ ) plus evidence for the reduction of  $\text{P}_4\text{W}^{\text{VI}}_{30}\text{Nb}_6\text{O}_{123}^{16-}$  by H<sub>2</sub> to form the well-known heteropolyblue complex,  $\text{P}_4\text{W}^{\text{VI}}_{26}\text{W}^{\text{V}}_4\text{Nb}_6\text{O}_{123}^{20-}$ .<sup>4,5</sup>

stoichiometry of formation of these scaled-up Ir(0) nanoclusters provided in eq 1. The significance of this expected finding, that the autocatalytic surface-growth mechanism applies to these scaled-up nanoclusters, is that all the insights afforded by this more general mechanism<sup>5,45</sup> should apply to the present, scaled-up nanoclusters, notably; the explanation for a preference toward magic number size nanoclusters, insights for controlling size and shape, and insights into how to rationally synthesize multimetallic nanoclusters in all their geometric isomers.<sup>35</sup>

### Conclusions

The present work recognizes the importance of, and directly addresses, the scale-up problem in transition-metal nanocluster science. A reproducible, scaled-up synthesis of polyoxoanion- and tetrabutylammonium-stabilized Ir(0) nanoclusters has been developed; the quantitative assessment of nanocluster stability based on catalytic activity has also been examined, an important but previously little addressed issue. The key results of this work are as follows: (i) the optimized, reproducible synthesis of  $880 \pm 10$  mg of polyoxoanion- and tetrabutylammonium-stabilized Ir(0) nanoclusters; (ii) elucidation of the best conditions for the scaled-up synthesis, namely, in propylene carbonate solvent, without cyclohexene, followed by isolation by precipitation with diethyl ether; (iii) demonstration of retention of 65% of the catalytic activity following isolation of the nanoclusters; (iv) demonstration of storage for 6 weeks as a solid under N<sub>2</sub> in a  $\leq 5$  ppm O<sub>2</sub> drybox with loss of  $\leq 15\%$  catalytic activity (and average loss of 2.5% activity/week); and (v) demonstration of the storage of the Ir(0) nanoclusters in solution for 30 days under 40 psig H<sub>2</sub> with no significant loss of catalytic activity. Also reported are the following: (vi) characterization of the nanoclusters by TEM, elemental analysis, GC, TGA/MS, IR, <sup>1</sup>H, and <sup>31</sup>P NMR, resulting in compositionally well-characterized nanoclusters of average molecular formula,  $[(n\text{-C}_4\text{H}_9)_4\text{N}]_{\sim 11000}\text{Na}_{\sim 5000}\text{Ir}_{\sim 2000}(\text{P}_4\text{W}_{30}\text{Nb}_6\text{O}_{123})_{\sim 1000}(\text{C}_4\text{H}_6\text{O}_3)_{\sim 5000}$ , such molecular formula rarely being reported in the nanocluster literature;<sup>1b,27</sup> (vii) strong evidence for the slow, continuous nucleation and then autocatalytic surface-growth mechanism for the formation of Ir(0) nanoclusters in propylene carbonate and all the insights this implies; and (viii) CS<sub>2</sub>-poisoning experiments allowing us to report the true TOF based

on the number of catalytically active sites and confirming that the soluble Ir(0) nanoclusters are the true catalysts in this system.

Significantly, the availability of near 1-g amounts of bottleable nanoclusters that can be stored for up to 6 weeks so that one can use them on-demand opens up all types of studies not previously possible, while greatly adding to the ease, efficiency, reproducibility, and reliability of those studies. One such group of studies is the determination of nanocluster surface compositions and structures under H<sub>2</sub>, N<sub>2</sub>, O<sub>2</sub>, H<sub>2</sub>O, and olefins, to start. Another is a detailed study of the kinetics and mechanism of olefin reduction, the initial results of which point to a little appreciated, H<sup>+</sup>-assisted hydrogenation mechanism.<sup>48</sup> Overall, it is hoped that the findings herein will go far toward identifying many of the key issues, as well as some of the preferred solutions, to the *scale-up problem* in transition-metal nanocluster science.

### Experimental Section

**Materials and Analytical Procedures.** Unless otherwise reported, all reaction solutions were prepared under oxygen- and moisture-free conditions using a Vacuum Atmospheres drybox ( $\leq 5$  ppm O<sub>2</sub> as continuously monitored by a Vacuum Atmospheres O<sub>2</sub>-level monitor).  $[(n\text{-C}_4\text{H}_9)_4\text{N}]_9\text{P}_2\text{W}_{15}\text{Nb}_3\text{O}_{62}$  was prepared according to our most recent procedure from Na<sub>12</sub>–[P<sub>2</sub>W<sub>15</sub>O<sub>56</sub>] and NbCl<sub>5</sub>.<sup>49</sup> The Na<sub>12</sub>[P<sub>2</sub>W<sub>15</sub>O<sub>56</sub>] was made from our recently optimized synthesis.<sup>50</sup>  $[(n\text{-C}_4\text{H}_9)_4\text{N}]_5\text{Na}_3[(1,5\text{-COD})\text{Ir} \cdot \text{P}_2\text{W}_{15}\text{Nb}_3\text{O}_{62}]$ , **1**, was prepared as previously described and its purity confirmed by <sup>31</sup>P NMR and elemental analysis.<sup>51</sup>

Cyclohexene (Aldrich, 99+%, stabilized with 0.01% 2,6-di-*tert*-butyl-4-methylphenol) was distilled from sodium metal under argon ( $\leq 99\%$  purity by GC) and stored in the drybox. Acetone (Burdick and Jackson, 0.26% H<sub>2</sub>O) was purged with argon for 30 min and transferred into the drybox. Propylene carbonate (Aldrich, 99.7%, anhydrous grade, water  $< 0.005$  wt %) was stored in the drybox over activated 5-Å molecular sieves. Diethyl ether (Aldrich, 99.9%, inhibitor-free, water  $< 0.03$  wt %) was used as received.

<sup>1</sup>H NMR and <sup>31</sup>P NMR were performed on a Varian Inova 300 spectrometer. Spectra were obtained in acetone-*d*<sub>6</sub> solution in oven-dried 5-mm-o.d. Spetra Tech NMR tubes at 22 °C and were referenced to benzene as an internal standard ( $\delta = 7.16$ ) for <sup>1</sup>H NMR and 85% H<sub>3</sub>PO<sub>4</sub> ( $\delta = 0$  ppm) for <sup>31</sup>P NMR.

(48) Lyon, D. K.; Aiken, J. D., III; Finke, R. G. Unpublished results.

(49) Weiner, H.; Aiken, J. D., III; Finke, R. G. *Inorg. Chem.* **1996**, *35*, 7905–7913.

(50) Hornstein, B. J.; Finke, R. G. *Inorg. Chem.* **2002**, *41*, 2720–2730.

(51) Pohl, M.; Lyon, D. K.; Mizuno, N.; Nomiya, K.; Finke, R. G. *Inorg. Chem.* **1995**, *34*, 1413.

Gas chromatography (GC) was performed using a Hewlett-Packard 5890 Series II GC with a FID detector equipped with either a Supelcowax 10 or a Supelco SPB-1 column coupled to a Hewlett-Packard 3395 integrator. Parameters were as follows:  $T_1 = 50\text{ }^\circ\text{C}$ ,  $t_1 = 3\text{ min}$ , ramp =  $10\text{ }^\circ\text{C/min}$ ,  $T_2 = 250\text{ }^\circ\text{C}$ ,  $t_2 = 1\text{ min}$ , injection volume = 4 or 2  $\mu\text{L}$ .

Thermal gravimetric analysis (TGA) was performed on 10–15-mg samples with a TA Instruments 2050 TGA equipped with a Balzers Thermo-Star quadrupole mass spectrometer. All analyses were carried out under  $\text{N}_2$  and heated from 30 to 600  $^\circ\text{C}$  at a rate of 5  $^\circ\text{C/min}$ .

Transmission electron microscopy (TEM) was performed at the University of Oregon with the expert assistance of Drs. Eric Schabtach and JoAn Hudson. Micrographs of the nanoclusters were obtained with a Phillips CM-12 microscope (with a 2.0-Å point-to-point resolution) operating at 100 keV. Nanocluster sizes were obtained from micrographs at 430 and 580 $\times$  magnification.

**General Ir(0) Nanocluster Synthesis Procedures.** In all cases, the Ir(0) nanoclusters were synthesized by “Standard Conditions” reactions as previously described using an in-house constructed hydrogenation apparatus.<sup>5,6,52</sup> (This consists of a Fischer–Porter pressure bottle connected to a hydrogen line with Swagelok quick-connects. The pressure in the Fischer–Porter bottle is then continuously monitored via an Omega pressure transducer that is connected to a PC by a White Box A/D converter.) Briefly,  $[(n\text{-C}_4\text{H}_9)_4\text{N}]_5\text{Na}_3[(1,5\text{-COD})\text{Ir}\cdot\text{P}_2\text{W}_{15}\text{Nb}_3\text{O}_{62}]$ , **1**, is weighed into a 5-mL vial in the drybox and dissolved in an appropriate amount of solvent. For reactions carried out with cyclohexene, the cyclohexene was added at this point with a 2.5-mL gastight syringe (see Table S1, Supporting Information, for the amounts of **1** and solvent used in each experiment). After the solid completely dissolved, this solution was transferred by disposable polyethylene pipet to a new 22  $\times$  175 mm borosilicate culture tube containing a new 5/16  $\times$  5/8 in. Teflon-coated stir bar. (The new culture tube for each experiment is an important part of the apparatus, one that avoids heterogeneous nucleation and, therefore, allows reproducible homogeneous nucleation during the nanocluster synthesis.<sup>4,5,53</sup>) The culture tube is then inserted into a 100-mL Fischer–Porter bottle, sealed, transferred out of the drybox, and attached to the hydrogenation apparatus referenced above. Next, the rapidly stirring solution is purged 15 times with  $\text{H}_2$  ( $40 \pm 1\text{ psig}$ , 15 s/purge) and the pressure is set to  $40 \pm 1\text{ psig H}_2$ . Formation of the catalyst is monitored directly by the evolution of cyclooctane as followed by GC as previously documented.<sup>4,52</sup> In all cases, the synthesis was stopped only after GC showed that  $1.0 \pm 0.1$  equiv of cyclooctane had evolved to ensure that the nanocluster catalyst was completely formed. (Monitoring the nanocluster formation reaction as directly as possible is an important, albeit infrequently performed, part of the best nanocluster syntheses.<sup>1a,1b,23,52</sup>)

After the nanocluster catalyst was completely formed, the Fischer–Porter bottle was returned to the drybox and the  $\text{H}_2$  pressure was released. Details of the catalyst isolation and storage are provided below.

**Synthesis of Ir(0) Nanoclusters Starting with 1.0 g of  $[(n\text{-C}_4\text{H}_9)_4\text{N}]_5\text{Na}_3[(1,5\text{-COD})\text{Ir}\cdot\text{P}_2\text{W}_{15}\text{Nb}_3\text{O}_{62}]$ .** In the drybox,  $1.00 \pm 0.01\text{ g}$  ( $1.76 \times 10^{-4}\text{ mol}$ ) of **1** was weighed into a 20-mL glass vial and dissolved in 15 mL of propylene carbonate added via a gastight syringe to give a clear amber solution. This solution was transferred into a new borosilicate culture tube containing a new 5/8  $\times$  5/16 in. Teflon-coated stir bar. The culture tube was then sealed inside of a Fischer–Porter bottle and a “Standard Conditions” reaction was carried out as described above. As the reaction proceeded, the solution became darker, changing from clear amber to dark amber to dark blue, indicative of heteropolyblue formation.<sup>54</sup> The Fis-

cher–Porter bottle was disconnected from the hydrogenation line and transferred back into the drybox, where the hydrogen pressure was released. The clear dark-blue reaction solution was transferred from the culture tube into a 600-mL beaker.

All still while in the drybox, 120 mL of diethyl ether was added dropwise over a period of 10 min via a polyethylene pipet to the stirred propylene carbonate solution of the Ir(0) nanoclusters. An additional 400 mL of diethyl ether was added in 30–50-mL portions to the mixture over 10 min to give the Ir(0) nanocluster product as a black viscous material at the bottom of the beaker. After vigorous stirring with a magnetic stir bar for 30 min, the mixture was left unstirred for 30 min to allow any suspended material to settle to the bottom of the beaker. The solvent was carefully decanted from the solid product and 150 mL of fresh diethyl ether was added in two 75-mL portions to further dry the sticky solid. After breaking up the large chunks with a metal spatula, the solid was allowed to settle for 30 min, and the solvent was carefully decanted. The black nanocluster material was then transferred by metal spatula into a 10-mL vial and dried under vacuum for 4 h at 25  $^\circ\text{C}$ . Isolated yield: 0.870–0.890 mg (82–85% based on the average molecular formula given below). The nanoclusters were stored double-bottled inside the drybox using a 10-mL push-cap vial for the inner bottle and a 1-L polypropylene bottle sealed with Parafilm for the outer bottle.

The Ir(0) nanoclusters were characterized by TEM, elemental analysis, GC, TGA/MS, IR,  $^1\text{H}$ , and  $^{31}\text{P}$  NMR. TEM images of the material re-suspended in acetonitrile show  $3.8 \pm 0.6\text{ nm}$  nanoclusters.<sup>26</sup> Elemental analysis of Ir(0) nanoclusters (Galbraith). Calcd for  $[(n\text{-C}_4\text{H}_9)_4\text{N}]_{11}\text{Na}_5\text{Ir}_2(\text{P}_4\text{W}_{30}\text{Nb}_6\text{O}_{123})\cdot(\text{C}_4\text{H}_6\text{O}_3)_5$ : C, 20.34; H, 3.67; N, 1.28; Ir, 3.19; P, 1.03. Found: C, 19.66; H, 3.65; N, 1.52; Ir, 3.01; P, 1.03. Combining the TEM and elemental analysis data yields an average molecular formula of  $[(n\text{-C}_4\text{H}_9)_4\text{N}]_{\sim 11000}\text{Na}_{\sim 5000}\text{Ir}_{\sim 2000}(\text{P}_4\text{W}_{30}\text{Nb}_6\text{O}_{123})_{\sim 1000}\cdot(\text{C}_4\text{H}_6\text{O}_3)_{\sim 5000}$ . Quantitative GC and TGA/MS were used to confirm the amount of residual propylene carbonate present (experimental details are provided in the Supporting Information). IR (KBr pellet, Figure S2, Supporting Information): 2959, 2930, 2875, 1784, 1638, 1479, 1378, 1090, 948, 920, 893, 781, and 644  $\text{cm}^{-1}$ .  $^1\text{H}$  and  $^{31}\text{P}$  NMR spectra were recorded in acetone- $d_6$  and are provided in Figures S3 and S4 of the Supporting Information. The yield ( $880 \pm 10\text{ mg}$ ) and initial catalytic activity ( $2.2 \pm 0.3\text{ mmol of H}_2/\text{h}$ ) are reproducible over three separate batches of pre-catalyst, **1**, and two different lots of propylene carbonate.

**CS<sub>2</sub> Poisoning of the Scaled-up Ir(0) Nanoclusters.** These experiments were carried out based on our literature procedure.<sup>28</sup> Details are provided in the Supporting Information.

**Smaller Scale Preparations of Ir(0) Nanoclusters Leading to the Optimized Synthesis for Scale-Up.** Experiments were carried out on 20–200-mg scales of **1** to determine the optimum synthesis conditions and procedure for the 1-g-scale experiments described above. All Ir(0) nanoclusters were synthesized under the “Standard Conditions” defined above. Experimental details concerning the amount of pre-catalyst, **1**, and the amount of reagents present in each reaction can be found in Table S1 of the Supporting Information.

**Storage of the In Situ Ir(0) Nanoclusters under 40 psig  $\text{H}_2$ .** Details of this storage procedure are provided in the Supporting Information.

**Testing the Catalytic Activity.** All catalyst activity measurements were performed on the previously described,<sup>4</sup> custom-built pressurized hydrogenation apparatus consisting of a pressurized Fischer–Porter bottle attached via Swagelok quick-connects to both a hydrogen supply (passed through water and oxygen scavengers) and connected to a pressure transducer. Unless otherwise stated, all reactions were carried out in the following manner and are based on our previously

(52) Aiken, J. D., III; Finke, R. G. *Chem Mater.* **1999**, *11*, 1035–1047.

(53) For evidence suggesting that heterogeneous nucleation can be a faster, lower energy pathway, at least in nanocluster formation reactions proceeding by diffusion-controlled steps, see: Strey, R.; Wagner, P. E.; Viisanen, Y. *J. Phys. Chem.* **1994**, *98*, 7748.

(54) (a) Pope, M. T. *Heteropoly and Isopoly Oxometalates*; Springer-Verlag: New York, 1983. (b) Pope, M. T. *Mixed-Valence Compounds*; Brown, D. B., Ed.; Reidel: Dordrecht, The Netherlands, 1980. (c) Buckley, R. I.; Clark, R. J. H. *Coord. Chem. Rev.* **1985**, *65*, 167.

established reaction conditions for catalyst lifetime experiments:<sup>52</sup> in a drybox, 5.0 mg of the solid catalyst was weighed into a disposable 10-mL glass vial. (For in situ experiments, a pre-selected amount of catalyst solution was added via a gastight syringe to a glass vial.) The material was then dissolved in the appropriate solvent (acetone or propylene carbonate) and 0.5 mL of cyclohexene was added with a 1.00-mL gastight syringe. In each experiment the total reaction solution volume was 3.00 mL. This solution was mixed with a disposable polyethylene pipet and then transferred into a new 22 × 175 mm culture tube containing a new 5/8 × 5/16 in. Teflon-coated magnetic stir bar. The culture tube was then placed inside the Fischer–Porter bottle, sealed, brought from the drybox, placed in constant temperature circulating water bath thermostated at 22.0 ± 0.1 °C, and attached to the hydrogenation apparatus via the quick-connects. Stirring was started (at >600 rpm) and the Fischer–Porter bottle was then purged 15 times with 40 psig H<sub>2</sub> (15 s/purge). The reaction vessel was then pressurized to 40 ± 1 psig H<sub>2</sub>, *t* = 0 was noted, and pressure vs time data were collected for 1 h at 1-min intervals.

The initial hydrogenation rate (see below) was calculated directly from the pressure vs time data for reactions carried out in propylene carbonate. Reactions carried out in acetone were corrected as before for the acetone vapor pressure that accumulates in the Fischer–Porter bottle over approximately the first half-hour of the reaction.<sup>45,55</sup>

For each synthesis of Ir(0) nanoclusters, the initial hydrogenation rate was determined either immediately after isolation or, for in situ samples, immediately after formation; the rates are reported in the “initial activity” column in Tables 2 and S1. The catalytic activity for all the samples, stored under the conditions described in Tables 2 and S1, were followed for up to 45 days with separate hydrogenation experiments. The activity over time was averaged and is given as the “average catalytic activity” column of Tables 2 and S1.

A control experiment was also carried out to show that the catalytic activity is first-order in catalyst concentration. This experiment rules out other mechanisms involving nanocluster reversible fragmentation to smaller, active species. The linear plot of activity vs amount of catalyst (Figure S6, Supporting Information) also demonstrates the absence of gas-to-solution mass-transfer effects.<sup>33</sup>

**Catalytic Data Treatment: The Initial-Rate Method.** Initial rates,  $(-dH_2/dt)_0$ , expressed in mmol of H<sub>2</sub>/h per 5.0 mg of catalyst were calculated from the pressure vs time data using the initial-rate method described elsewhere.<sup>56</sup> Briefly, the data were fit to a polynomial expression using Kaleida-Graph V. 3.51. At *t* = 0,  $(-dH_2/dt)_0$  is the first-order coefficient of the polynomial fit and reproduced below for the function *f* of *t*, *f*(*t*).

$$f(t) = C_1 + C_2 t + C_3 t^2 + C_4 t^3 \dots$$

$$df/dt = C_2 + 2C_3 t + 3C_4 t^2 \dots$$

$$\text{At } t = 0, df/dt = C_2 \text{ and since } (-dH_2/dt)_0 = df/dt,$$

$$\text{it follows that } (-dH_2/dt)_0 = C_2, \text{ the initial rate}$$

The initial rates determined in this manner were, for all experiments, within 3–5% of initial rates calculated from fitting the first 25% of the data to a straight line. Although both methods give similar values, those obtained from the more rigorous polynomial fits are reported. For isolated catalysts, 5.0 ± 0.3 g was used in each hydrogenation reaction and the rate was corrected to 5.0 mg of catalyst. (The initial

rate shows a first-order dependence upon catalyst concentration, so the correction is simply linear.) For the in situ studies, a preselected volume of solution was added to test the catalytic activity. It was assumed that the entire amount of pre-catalyst, **1**, was converted to catalyst in the nanocluster formation reaction. The concentration of this solution, expressed as mg of catalyst/mL of reaction solution, was used to calculate the amount of catalyst added to the hydrogenation reactions. These observed rates were then corrected to 5.0 mg of catalyst just as done for experiments with isolated solid.

**Experiments Verifying the Autocatalytic Surface-Growth Mechanism of Ir(0) Nanocluster Formation in Propylene Carbonate.** Details of the H<sub>2</sub> uptake apparatus and the procedure are provided in the Supporting Information.

**Acknowledgment.** Drs. Jody Aiken, III, and Frank Müller are acknowledged for performing early survey experiments leading to the use of propylene carbonate as a preferred solvent for these scale-up studies. We thank Professor Steven H. Strauss for allowing us to use his high-vacuum line for the H<sub>2</sub> gas-uptake experiments described herein and Dr. Aiken for performing those experiments. Professor C. Winter at Wayne State is thanked for sharing his findings on the air sensitivity of Cu nanoparticles being used in his research, a disclosure which caused us to rethink the air sensitivity of the Ir(0) nanoclusters reported herein. Financial support was provided by the Department of Energy, Chemical Sciences Division, Office of Basic Research, via Grant DOE FG06-089ER13998.

**Supporting Information Available:** Figure S1: Plot of cyclooctane evolved vs time that accompanies the conversion of the pre-catalyst, [(1,5-COD)Ir·P<sub>2</sub>W<sub>15</sub>Nb<sub>3</sub>O<sub>62</sub>],<sup>8-</sup> to 3.8 ± 0.6 nm Ir(0) nanoclusters. Figure S2: IR (KBr pellet) of the scaled-up Ir(0) nanoclusters isolated from propylene carbonate by precipitation with Et<sub>2</sub>O. Figure S3: <sup>1</sup>H NMR (acetone-*d*<sub>6</sub>) of a saturated solution of Ir(0)-polyoxoanion nanoclusters isolated from propylene carbonate by precipitation with diethyl ether. Figure S4: (a) <sup>31</sup>P NMR of 90% pure [(*n*-C<sub>4</sub>H<sub>9</sub>)<sub>4</sub>N]<sub>9</sub>[P<sub>2</sub>W<sub>15</sub>Nb<sub>3</sub>O<sub>62</sub>] in acetone-*d*<sub>6</sub>; (b) <sup>31</sup>P NMR spectrum of isolated polyoxoanion- and tetrabutylammonium-stabilized Ir(0) nanoclusters redissolved in acetone-*d*<sub>6</sub>. Text: Experimental procedure for the CS<sub>2</sub> poisoning of the scaled-up Ir(0) nanoclusters. Figure S5: Plot of the relative rate vs mol of CS<sub>2</sub>/mol of total Ir(0) for the hydrogenation of cyclohexene by the scaled-up Ir(0) nanoclusters. Figure S6: Plot of activity vs mg of catalyst demonstrating a first-order dependence on catalyst concentration and showing the absence of H<sub>2</sub> mass-transfer limitations under the reaction conditions. Figure S7: TEM of the deactivated Ir(0) nanoclusters after storage as a solid in the drybox for >253 days. Figure S8: Plot of the activity vs age for four separate syntheses of Ir(0) nanoclusters isolated from acetone by solvent evaporation. Figure S9: Plot of the activity vs age for five separate syntheses of Ir(0) nanoclusters isolated from propylene carbonate by precipitation with diethyl ether. Text: Description of the hydrogen gas uptake apparatus and the procedure used to determine the H<sub>2</sub>/Ir stoichiometry in propylene carbonate. Figure S10: The gas-uptake apparatus used to measure the Ir/H<sub>2</sub> stoichiometry. Figure S11: Plot showing uptake of 3.6 ± 0.4 equiv of H<sub>2</sub>/mol of Ir beginning with **1** in propylene carbonate at 22.5 °C. Figure S12: GC of the reaction mixture from the H<sub>2</sub> gas-uptake experiment beginning with 103.4 mg of **1** in 2.0 mL of propylene carbonate. Table S1: Complete summary of Ir(0) nanocluster synthesis conditions and catalytic activity. Text: Effect of storage conditions on in situ Ir(0) nanoclusters' activity: H<sub>2</sub> vs N<sub>2</sub> atmosphere. Text: Quantitative GC experiments to confirm the amount of residual propylene carbonate in the scaled-up Ir(0) nanocluster product (PDF). This material is available free of charge via the Internet at <http://pubs.acs.org>.

CM020856Y

(55) The pressure due solely to the acetone vapor was determined in a standard conditions hydrogenation experiment in which, however, the catalyst was omitted. The resultant acetone vapor pressure value was subtracted from the raw experimental data before the initial hydrogenation rate,  $(-dH_2/dt)_0$ , was determined (see elsewhere for details<sup>45</sup>).

(56) Wilkins, R. G. *Kinetics and Mechanism of Reactions of Transition Metal Complexes*, 2nd ed.; VCH: New York, 1991.